

# The Goldstone mode and resonances in the fluid interfacial region

A. O. Parry<sup>1</sup> and C. Rascón<sup>1,2\*</sup>

**The development of a molecular theory of inhomogeneous fluids and, in particular, of the liquid–gas interface has received enormous interest in recent years; however, long-standing attempts to extend the concept of surface tension in mesoscopic approaches by making it scale dependent, although apparently plausible, have failed to connect with simulation and experimental studies of the interface that probe the detailed properties of density correlations. Here, we show that a fully microscopic theory of correlations in the interfacial region can be developed that overcomes many of the problems associated with simpler mesoscopic ideas. This theory originates from recognizing that the correlation function displays, in addition to a Goldstone mode, an unexpected hierarchy of resonances that constrain severely its structural properties. Indeed, this approach allows us to identify new classes of fully integrable models for which, surprisingly, the tension, density profile and correlation function can all be determined analytically, revealing the microscopic structure of correlations in all generalized van der Waals theories.**

Interfaces, for example between liquids and gases or between solids and liquids, are ubiquitous in nature, playing crucial roles across all of biology and in modern technologies from oil recovery to microfluidics. The key ingredient in our understanding of them is the nature of the surface tension: the macroscopic energy cost of separating coexisting fluid phases. Indeed, at large scales, the interface behaves like a taut drum skin, with the surface tension acting always to minimize the exposed surface area. However, it has also long been recognized that the surface tension provides insight into the microscopic world, since it arises directly from the imbalance between the attractive intermolecular forces either side of the interface. It was van der Waals who first developed a microscopic theory that not only predicted the coexistence of liquid and gas phases, but also the structure of the interface separating them, specifically that the change from a high-density liquid to a low-density gas does not occur abruptly, but smoothly over a molecular scale. The modern statistical mechanical theory of interfaces is based on a marriage between these large-scale and microscopic approaches. However, this union has not always been easy and has been the subject of many controversies.

Consider an interface situated near the  $z=0$  plane separating coexisting bulk liquid and gas phases below a critical temperature,  $T_c$ . Three microscopic quantities of particular importance are the equilibrium density profile,  $\rho(z)$ , the two-dimensional Fourier transform of the density–density pair correlation function in the direction along the interface,  $G(z, z'; q)$ , and its integral,  $S(z; q) = \int dz' G(z, z'; q)$ , which defines the local structure factor, where  $z$  and  $z'$  are the positions perpendicular to the interface, and  $q$  is the wave number parallel to it. Integrals of  $G(z, z'; q)$  are directly related to the intensity measured in scattering studies, while  $S(z; q)$  is of thermodynamic importance since, at  $q=0$ , it is equal to the local compressibility (the derivative of the local density with respect to chemical potential). A key insight in modern statistical mechanical theory is that, if the interface is not subject to external forces, the density–density correlation function must contain a Goldstone mode in the long-wavelength limit, since the interface can be translated without cost of energy<sup>1–3</sup>. Thus, at small wave vectors

(well below the scale of the inverse bulk correlation length), it is well established from exact sum rules that the correlation function (and hence  $S(z; q)$ ) diverges as  $G(z, z'; q) \approx \rho'(z)\rho'(z')/\beta\sigma q^2$ , with  $\beta = 1/k_B T$  (hereafter set to 1),  $k_B$  is the Boltzmann constant,  $T$  is the temperature,  $\rho'(z)$  is the derivative of the density profile and  $\sigma$  is the surface tension. We refer to this divergence as the Wertheim–Weeks Goldstone mode (WWGM)<sup>3,3</sup>. At these long wavelengths, there is a happy marriage with the picture of the interface as a taut drum skin. This is explicit in the mesoscopic capillary-wave description of the interface, which models it as a position-dependent height  $h(\mathbf{x})$  with an energy cost  $H[h] = \frac{\sigma}{2} \int d\mathbf{x} (\nabla h)^2$ , that is, surface tension multiplied by area (ref. 4). Equipartition immediately implies that the Fourier transform of the height–height correlation function behaves as  $1/\sigma q^2$ . This not only tallies perfectly with the WWGM, but has the profound consequence that the width of the interface is broadened due to its thermal fluctuations<sup>4</sup>, a feature that has been visualized directly in colloid–polymer mixtures<sup>5</sup>.

What happens beyond the Goldstone mode (that is, at higher wave vectors) has received a great deal of attention in recent decades<sup>6–20</sup>. One popular approach borrows ideas from the theory of membranes<sup>21</sup> and extends the capillary-wave model by including a higher-order term,  $\frac{K}{2} \int d\mathbf{x} (\nabla^2 h)^2$ , arising from the curvature of the interface, where  $K$  is a rigidity. Clearly, this alters the expression for the height–height correlation function to  $1/(\sigma q^2 + Kq^4)$ . With a positive rigidity, this approach has the advantage of eliminating the need to impose an explicit cut-off, and was hoped to be a shortcut to determining the properties of  $G(z, z'; q)$  and  $S(z; q)$  (ref. 6). This plausible approach is, however, plagued with problems. Long-range dispersion forces introduce non-analytic contributions<sup>7,10</sup>, implying that  $K$  is not well defined. For systems with short-range forces, commonly used in simulation studies, attempts to identify  $K$  have also run into numerous difficulties. For example, unlike  $\sigma$ , the value of  $K$  is unsatisfactorily sensitive to how  $h(\mathbf{x})$  (that is, the local separation of liquid and gas) is defined microscopically. Moreover, simple definitions, such as those used in density functional theories (DFTs) of wetting, fail because they lead to unphysical negative values for  $K$  (refs 8,14). In addition, it is now apparent that, even with a positive  $K$ ,

<sup>1</sup>Department of Mathematics, Imperial College London, London, UK. <sup>2</sup>GISC, Departamento de Matemáticas, Universidad Carlos III de Madrid, Leganés, Spain. \*e-mail: [carlos.rascon@uc3m.es](mailto:carlos.rascon@uc3m.es)

this approach is not a shortcut to determination of the underlying microscopic observables  $G(z, z'; q)$  and  $S(z; q)$ . In fact, the opposite is true: we need to know  $G(z, z'; q)$  to define a rigidity if we wish to extend capillary-wave theory<sup>20</sup>. In this paper, we shall show in fact that both  $G(z, z'; q)$  and  $S(z; q)$  contain information occurring at higher wave vectors that cannot possibly be encapsulated using a rigidity and that does not rely on the definition of an interface position.

### Existence of resonances

Let us first try to identify the properties of  $S(z; q)$  at higher wave vectors by using general principles. We specialize to systems with short-range intermolecular forces (for example, finite range or exponentially decaying) and specify the bulk properties first. Far from the interface, the density and structure factor take their bulk liquid ( $b=1$ ) or bulk gas ( $b=g$ ) values,  $\rho_b$  and  $S_b(q)$ , respectively. The bulk structure factor is the three-dimensional Fourier transform of the density–density correlation function, which we assume decays monotonically in the liquid as well as the gas phase in standard Ornstein–Zernike fashion,  $G_b(r) \approx e^{-\kappa r}/r$ , where  $r$  is the distance (ref. 22). Here,  $\kappa$  is the inverse of the appropriate bulk liquid or gas correlation length  $\xi$ , identified formally from the condition  $C_b(i\kappa) = 0$ , where  $C_b(q) = 1/S_b(q)$  is the three-dimensional Fourier transform of the bulk direct correlation function and  $i$  is the square root of  $-1$ . The bulk correlation length also determines the asymptotic exponential decay of the density profile; for example, on the liquid side,  $\rho(z) - \rho_1 \approx e^{-\kappa z}$ , where in general, the correction terms are simply higher powers of  $X = e^{-\kappa z}$ . We do not need to specify the details of the broadening of the interface, which would appear in the coefficients of the expansion, since this has no influence on the location of the resonances. In DFT, the local structure factor can be determined from the solution of refs 23,24:

$$\int dz' C(z, z'; q) S(z'; q) = 1 \quad (1)$$

which is the integral of the usual Ornstein–Zernike equation for  $G(z, z'; q)$ . Here,  $C(z, z'; q)$  is the two-dimensional Fourier transform of the direct correlation function of the inhomogeneous fluid, which is determined as the second functional derivative of the intrinsic Helmholtz free-energy functional.

In an earlier paper<sup>18</sup>, we showed how the asymptotic decay of  $S(z; q)$  each side of the interface ( $|z| \rightarrow \infty$  at fixed  $q$ ) can be determined exactly, ignoring minor three-body contributions, as

$$S(z; q) = S_b(q) + \frac{\Delta \rho \rho'(z)}{q^2 \sigma_b(q)} + \dots \quad (2)$$

where  $\Delta \rho = \rho_1 - \rho_g$  and  $q^2 \sigma_b(q) \propto C_b(q) C_b(i\sqrt{\kappa^2 - q^2})$ . Thus, the wave-vector dependence of the leading-order asymptotic decay is different on the liquid and gas sides, which is not at all explicable using one rigidity. The coefficients  $\sigma_b(q)$  are determined exclusively by bulk quantities and show a rich temperature dependence, consistent with that of the total (integrated) structure factor as measured in simulation studies of truncated Lennard–Jones systems, as shown in Fig. 1. Although this agreement is encouraging, many important questions remain unanswered. Do the asymptotic tails of  $S(z; q)$  truly represent the interfacial behaviour? What happens nearer the interface, and how do the asymptotic behaviours swap between the liquid and gas sides? How are the two coefficients  $\sigma_b(0)$  related, if at all, to the surface tension? How do we guarantee that we recover the WWGM as  $q \rightarrow 0$ ?

Key to answering these questions and developing a fully microscopic description of correlations in the interfacial region is

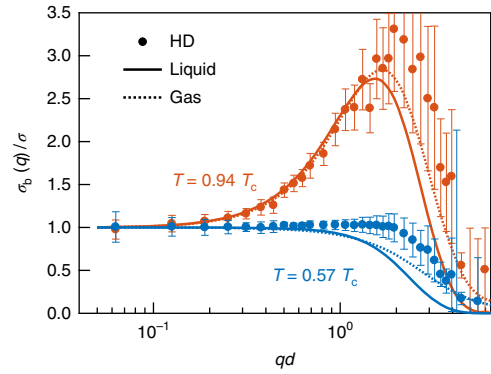


**Fig. 1 | Comparison of  $\sigma_l(q)$  and  $\sigma_g(q)$  with  $\sigma_{HD}(q)$ .** The  $\sigma_{HD}(q)$  is obtained from an excess-like contribution to the total (integrated) structure factor,  $S^{ex}(q) = (\Delta \rho)^2 / q^2 \sigma_{HD}(q)$ , after a background term is extracted (approximately, the volumes of the liquid and gas multiplied by their respective bulk structure factor). Data are taken from simulation studies involving  $5 \times 10^5$  truncated Lennard–Jones particles with core diameter  $d$  at two representative temperatures<sup>15</sup>. Errors represent standard deviations. The coefficients  $q^2 \sigma_b(q) \propto C_b(q) C_b(i\sqrt{\kappa^2 - q^2})$  were calculated using only simulation data results for the bulk liquid and gas quantities, respectively.

recognizing that the local structure factor must, in general, exhibit resonances each side of the interface. More specifically, the formalism of DFT, which is exact in principle, implies that, in addition to the Goldstone mode at  $q=0$ , there must also be resonances at specific wave vectors. The presence of these resonances can be understood fairly easily by noting that, in general, each side of the interface, the general solution for  $S(z; q)$  can be written as a sum of two expansions: one in the variable  $X$  (that is, similar to the density profile), which can be obtained by expanding  $C(z, z'; q)$  about, for example, the liquid density, and a second expansion defined as the solution to equation (1), but with the right-hand side set to zero. The leading term of this second series decays as  $e^{-\kappa_q z}$ , where  $\kappa_q = \sqrt{\kappa^2 + q^2}$ , and can be directly related to the correlation function  $G(0, z; q)$  where the origin is conveniently chosen to correspond to the maximum of  $\rho'(z)$  (refs 18,25) (see also the Supplementary Information). Note that this is not a definition of the interface position, but merely a convenient choice of the origin of coordinates. This means that, on the liquid side,  $S(z; q)$  must have resonances—that is, the amplification of a particular exponentially decaying term—when  $\kappa_q$  is an integer multiple of  $\kappa$ ; that is, when the wave vector satisfies  $\xi q = \sqrt{3}, \sqrt{8}, \sqrt{15}, \dots$ . Similar resonances occur on the gas side of the interface at slightly different  $q$  values, since the correlation length of the gas is different. The existence of these resonances severely constrains the relationship between the structure factor and correlation function and, in many circumstances, is sufficient to determine both exactly, as we shall show below.

### An example: square-gradient theory

As a first example, we consider a mean-field square-gradient theory based on the model grand potential functional<sup>23</sup>

$$\Omega[\rho] = \int dr \left[ \frac{f}{2} (\nabla \rho)^2 + \phi(\rho) \right] \quad (3)$$

where  $f$  is a constant and  $\phi(\rho)$  is a double-well potential describing the coexistence of liquid and gas phases below  $T_c$ . Thermodynamic equilibrium requires that  $\phi(\rho_g) = \phi(\rho_l)$ , while the bulk structure factor is  $S_b(q) = 1/(\phi''(\rho_b) + f q^2)$  and identifies  $\xi^2 = f/\phi''(\rho_b)$ . Hereafter, a prime denotes differentiation of a function with respect to its argument. For

convenience, we define  $\Delta\phi(\rho) \equiv \phi(\rho) - \phi(\rho_b)$ , which will be useful later. Minimization of the grand potential functional (equation (3)) leads to the well-known Euler–Lagrange equation for the density profile  $f\rho''(z) = \phi'(\rho)$  and, in turn, to  $\sigma = f \int dz \rho'(z)^2$ . Although this mean-field approach does not account for the capillary-wave broadening of the interface, we will see that this plays no role in the discussion of the resonances. We now consider the general class of potentials  $\phi(\rho)$  that are analytic except, perhaps, at the critical density  $\rho_c = (\rho_l + \rho_g)/2$ , where we just impose continuity and  $\phi'(\rho_c) = 0$ . For simplicity, we specialize initially to systems with a liquid–gas (Ising-like) symmetry; the effect of asymmetry is accounted for later. We can classify all such potentials via the coefficients  $u_n$  appearing in the expansion about the bulk liquid density; thus, for  $\rho > \rho_c$ , we write  $\phi'(\rho) = f\kappa^2 \delta\rho(1 + u_3 \delta\rho/\Delta\rho + u_4(\delta\rho/\Delta\rho)^2 + \dots)$  with  $\delta\rho = \rho - \rho_l$ . A similar expansion exists about the gas density for  $\rho < \rho_c$ . In this class of models, the resonances determine that the local structure factor must always be of the form (see Supplementary Information)

$$S(z; q) = S_b(q) \left( 1 + \lambda \sum_{n=1}^{\infty} \frac{\sigma}{\sigma_n} \mathcal{R}_n(z; q) \right) \quad (4)$$

where  $\lambda = \Delta\rho/\rho'(0)S_b(0)$  is a constant and  $\sigma_n$  are generalized tensions. The leading term

$$\mathcal{R}_1(z; q) = \frac{\rho'(0)\rho'(z)}{\sigma q^2} \quad (5)$$

describes the asymptotic decay (as in equation (2)), while for  $n > 1$

$$\mathcal{R}_n(z; q) = \frac{G(0, z; q) - G(0, z; \sqrt{n^2 - 1} \kappa)}{1 - \frac{q^2 \xi^2}{n^2 - 1}} \quad (6)$$

is the isolated contribution from each resonance.  $S(z; q)$  has a maximum at  $z = 0$  and decays towards its bulk value as  $|z|$  increases, as expected. Note that  $\mathcal{R}_1(z; q)$  contains an explicit Goldstone mode divergence, while both the numerator and denominator of  $\mathcal{R}_n(z; q)$  vanish at  $\xi q = \sqrt{n^2 - 1}$ , which also has an implicit Goldstone mode divergence contained in  $G(0, z; q)$ . The explicit Goldstone mode and resonances are weighted by  $\sigma_n$ , with  $\sigma_1 = f\kappa(\Delta\rho)^2/2u_3$  (equivalent to  $\sigma_b(0)$ ), which, at low temperatures, is larger than  $\sigma$  (ref. 18). Higher coefficients are determined similarly (see Supplementary Information) and satisfy the useful summation condition  $1/\sigma = 1/\sigma_1 + 1/\sigma_2 + \dots$ , ensuring that  $S(z; q)$  has the required WWGM divergence  $S(z; q) \approx \Delta\rho\rho'(z)/\sigma q^2$  at small wave vectors. Equation (4) describes the general form of the structure factor throughout the interfacial region, encompassing both the large-distance behaviour (fixed  $q$ ,  $|z| \rightarrow \infty$ ) and the WWGM divergence (fixed  $z$ ,  $q \rightarrow 0$ ). A number of immediate implications follow:

(1) In general, the leading-order exponential decay of  $S(z; q)$  comes from the explicit Goldstone mode term  $\mathcal{R}_1(z; q)$ . However, higher-order exponentials include corrections at the resonances. For example, at  $\xi q = \sqrt{3}$ , the next higher-order term in  $S(z; q)$  decays as  $|z|e^{-2\xi|z|}$ , whose coefficient is determined by the sign of  $(u_4 - 2u_3^2/9)$ .

(2) The presence of just one resonance means that, even with an idealized Ising symmetry, there is no consistent separation of both  $S(z; q)$  and  $G(0, z; q)$  into bulk and excess terms, as has been routinely assumed.

(3) For a given  $q$ , the local structure factor is maximal at the origin (that is, where  $\rho'(z)$  also has a maximum), and its value  $S(0; q)$  is shielded from information contained in the correlation function. To see this, suppose that  $G(0, 0; q) \approx \rho'(0)^2/\sigma q^2 + \mathcal{C}$ , containing the WWGM and an additive constant  $\mathcal{C}$ . This could be generated by the

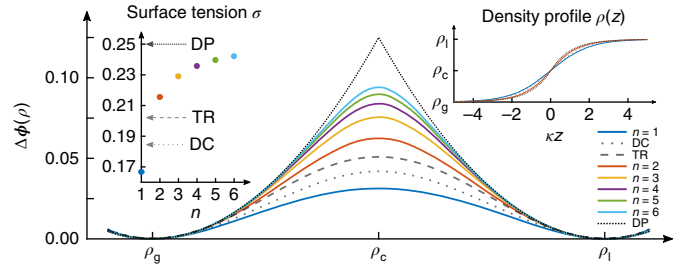


**Fig. 2 | Results for model potentials whose  $S(z; q)$  displays a single resonance at  $\xi q = \sqrt{n^2 - 1}$ .** The potentials  $\Delta\phi(\rho)$  are measured in units of  $f\kappa^2(\Delta\rho)^2$ . Insets show the corresponding density profiles and tensions (in units of  $f\kappa(\Delta\rho)^2$ ). The case where  $n=1$  (a pure Goldstone mode divergence) corresponds to the standard Landau quartic potential. As  $n$  increases, the potential approaches the form of a double parabola (DP). The double-cubic (DC) and trigonometric (TR) potentials are also shown.

low- $q$  behaviour of a background contribution, or as an expansion arising if we suppose the surface tension in the WWGM is replaced with  $\sigma + Kq^2$ . Substitution into equation (4) determines that

$$\frac{S(0; q)}{S_b(q)} \approx 1 + \frac{\Delta\rho\rho'(0)}{\sigma q^2 S_b(0)} \quad (7)$$

which is independent of  $\mathcal{C}$ . This tells us a number of things. First, that the approximate, non-additive, separation (equation (7)) will be accurate for a wide class of models; it is indeed exact for the standard quartic Landau potential<sup>14</sup>. Second, that the corrections to the WWGM are determined by properties of the bulk structure factor (or bulk direct correlation function) throughout the interfacial region, and not just in the tails of  $S(z; q)$ , which explains the close agreement between the effective wave-vector-dependent surface tension,  $\sigma_{\text{HD}}(q)$ , where the subscript ‘HD’ refers to Höfling and Dietrich<sup>15</sup>, and  $\sigma_b(q)$  in Fig. 1. Finally, that the leading-order correction to the WWGM divergence in  $S(0; q)$  is unrelated to the leading-order correction in the WWGM divergence of the correlation function. This means that it is impossible to infer directly the value of any rigidity in  $G(0, 0; q)$  from the structure factor.

(4) Integration of equation (4) over a macroscopic interval  $[-L/2, L/2]$  determines a similar exact result for the total structure factor  $S_{\text{total}}(q)$  as a sum of the resonances (see Supplementary Information). From this, it follows that  $S_{\text{total}}(q)$  is always well approximated by

$$\frac{S_{\text{total}}(q)}{S_b(q)} \approx L + \frac{(\Delta\rho)^2}{\sigma q^2 S_b(0)} \quad (8)$$

This result does not rely on the density profile and, therefore, is unlikely to be affected by capillary-wave fluctuation effects.

### Counting the resonances

We can take the theory further and classify the potentials  $\phi(\rho)$  according to the presence or absence of resonances (see Supplementary Information). For example, when  $u_4 = 2u_3^2/9$ , the resonance at  $\xi q = \sqrt{3}$  is missing, and further setting  $u_5 = 0$  removes the next resonance at  $\xi q = \sqrt{8}$ . Alternatively, we can be more stringent and consider the class of single-resonance models (SRMs) containing just one resonance at  $\xi q = \sqrt{n^2 - 1}$  for which  $S(z; q) = S_b(q)(1 + \lambda\mathcal{R}_n(z; q))$ . Such SRM potentials can be determined and are shown in Fig. 2.

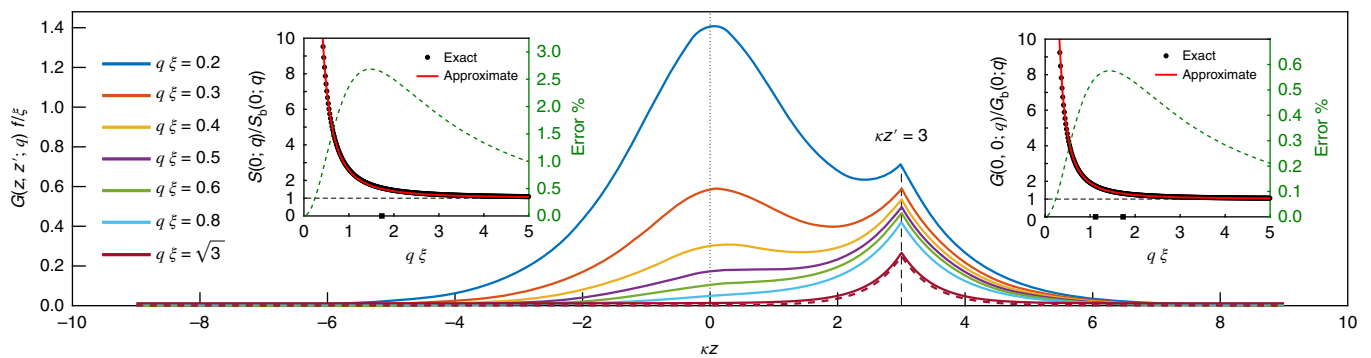


**Fig. 3** |  $G(z, z'; q)$  for the double-cubic potential for different wave vectors  $q$  and fixed  $\kappa z' = 3$ . A prominent Goldstone mode is apparent near the origin at small wave vectors. For larger values of  $q$ ,  $G(z, z'; q)$  becomes more bulk-like and is almost indistinguishable from it (dashed lines) for  $q\xi = \sqrt{3}$  (the first resonance in  $S(z; q)$ ). Insets show exact results for  $S(0; q)$  and  $G(0, 0; q)$  (explicit expressions can be found in the Supplementary Information) compared with the multiplicative approximations, equations (7) and (9), respectively. These remain accurate over the whole range of wave vectors. For example, the error (green dashed lines) is about 2.5% maximum for  $S(0; q)$  and only about 0.6% maximum for  $G(0, 0; q)$ . The squares in the horizontal axes locate the resonances, which do not show any noticeable feature in the functions  $S(0; q)$  or  $G(0, 0; q)$ .

For  $n=1$  (a model with no resonances),  $\phi(\rho)$  has a quartic expansion with coefficients  $u_3=3$  and  $u_4=2$  and corresponds precisely to the standard potential of Landau theory,  $\phi = -t(\rho - \rho_c)^2 + u(\rho - \rho_c)^4$ , with  $t \propto T_c - T$ . In this case, equations (7) and (8) are exact, while for higher  $n$ , the right-hand side of both equations are lower bounds. For  $n=2$  (a model with only one resonance at  $\xi q = \sqrt{3}$ , in addition to the Goldstone mode), the potential is similarly quartic, but the coefficients are  $u_3=0$  and  $u_4=-4$ . The potential for SRMs for higher  $n$ , however, no longer truncate (see Supplementary Information). In the limit  $n \rightarrow \infty$ , the potential recovers a double parabola (in which all the coefficients  $u_n$  are zero), and the single resonance in  $\mathcal{R}_\infty(z; q)$  disappears, since it occurs at infinite wave number. Indeed, apart from the Landau quartic potential, this is the only other model for which the structure factor does not exhibit resonances. This is all the more surprising given that these two limiting SRM potentials are the only ones for which  $G(z, z'; q)$  and  $S(z; q)$  have been studied.

In the absence of such fine tuning, we must expect that  $\sigma_1 \neq \sigma$  and that all resonances are present in  $S(z; q)$ . However, at low temperatures,  $\xi$  is molecularly small, so it may not be possible to reach wave vectors where the explicit resonant decay of  $S(z; q)$  is observable. As the temperature is increased towards  $T_c$ , the correlation length increases, which exposes the resonances (see Supplementary Information).

### Fully integrable models

By considering the occurrence of the resonances, we can identify models that are fully analytically integrable; that is, potentials for which the profile, surface tension,  $G(z, z'; q)$  and  $S(z; q)$  can be determined analytically. Only one non-trivial example of this was known previously, corresponding to the Landau quartic potential for which Zittartz first determined  $G(z, z'; q)$  using spectral methods<sup>1</sup>. The only other example is the double-parabola model, which similarly does not contain resonances<sup>14</sup>.

However, our approach identifies many model potentials (in fact, an infinite number) that are fully integrable, all of which include resonances. Among these are the SRM with  $n=2$  and the trigonometric potential  $\Delta\phi(\rho) \propto \sin^2(\pi(\rho - \rho_g)/\Delta\rho)$ . This latter potential generates an infinite number of resonances at  $\xi q = \sqrt{n^2 - 1}$  for even  $n$ . However, the example that is most pertinent to fluids, away from the critical regime, is the double-cubic model with  $u_3=2$  (and all other coefficients zero). This potential is particularly useful because the value of  $\sigma_1 = f(\Delta\rho)^2 \kappa / 4$  is larger than the equilibrium tension  $\sigma$  as applied to real fluids at low temperatures<sup>18</sup>. This model contains

all resonances of  $S(z; q)$  and can be readily generalized to encompass liquid–gas asymmetry. The behaviour of  $G(z, z'; q)$  for this double-cubic potential is shown in Fig. 2 and illustrates the smooth development of the WWGM divergence as the wave vector is reduced. The analytical results show that  $G(z, z'; q)$  also contains a new resonance at  $\xi q = \sqrt{5/4}$  when the particles are on the same side of the interface (see Supplementary Information). Similar behaviour is found in other integrable models. For example, in the SRM with  $n=2$ , the correlation function (like the structure factor) contains a Goldstone mode and a single resonance at  $\xi q = \sqrt{3}$ . We have shown that, for more general types of potential, the correlation function must have resonances when  $\xi q = \sqrt{(m^2 - 4)/4}$  for  $m = 3, 4, \dots$ ; again when both particles are on the same side of interface. This includes the same resonances contained in  $S(z; q)$  (when  $m$  is even) and a new set occurring at  $\xi q = \sqrt{5/4}, \sqrt{21/4}, \dots$  (when  $m$  is odd).

The results for  $G(z, z'; q)$  show that, similar to the robust approximation, equation (7), the correlation function at the interface is always well approximated by

$$\frac{G(0, 0; q)}{G_b(0; q)} \approx 1 + \frac{\rho'(0)^2}{\sigma q^2 G_b(0; 0)} \quad (9)$$

Here,  $G_b(z; q) = e^{-\kappa_q |z|} / 2f\kappa_q$  is the two-dimensional Fourier transform of the bulk correlation function (along the  $x$ – $y$  plane), so that  $G_b(0; q)$  corresponds to the two-dimensional Fourier transform when the particles are co-planar. Indeed, equation (9) is the exact result for the Landau quartic potential and trigonometric model. Thus, at the origin (and only at the origin), the approximate rule of factoring out a bulk background and a multiplicative correction to the Goldstone mode describes accurately the correlation function and structure factor over the whole range of wave vectors (see Fig. 3).

### The Sullivan model and the bulk enhancement effect

As a second example, we present results for the well-known Sullivan DFT model of the free interface, based on a local approximation of the repulsive hard-sphere contribution and a non-local, mean-field, treatment of an attractive Yukawa intermolecular potential, where  $R$  is the range and  $\alpha$  the integrated strength<sup>26–29</sup>. This more microscopic description of the interfacial region will allow us to see some limitations of square-gradient theory and finally introduce liquid–gas asymmetry. We will in fact consider a broad class of Sullivan-like models in which the model chemical potential for bulk

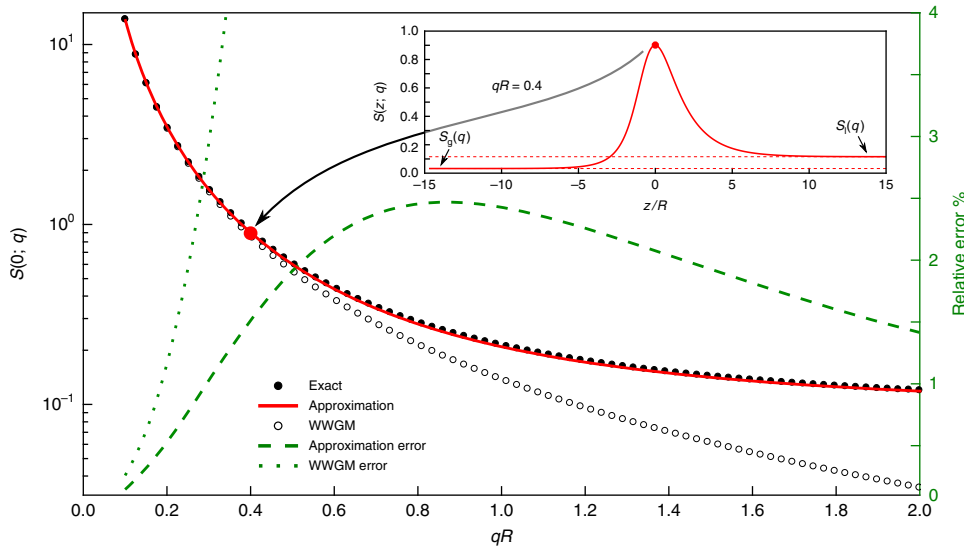


**Fig. 4 | Sullivan model results for  $S(0;q)$  using the Carnahan–Starling equation of state for hard spheres.** We chose  $T/T_c = 0.72$ , for which the ratio of the bulk liquid and gas correlation lengths  $\xi_l^T/\xi_g^T \approx 2.1$ , representing strong liquid–gas asymmetry. The superscript T denotes the true correlation length defined from the exponential decay of  $G(r)$ . The structure factor is measured in units of  $R^2/\alpha$ . The main graph illustrates the extraordinary accuracy of the approximation, equation (14) (red line), compared with the numerical solution of the Ornstein–Zernike equation (black circles) over the whole range of wave vectors. As expected, the WWGM (open circles) is valid only when  $q$  is much smaller than the inverse of the bulk correlation lengths. Relative errors are shown in green. The error of the approximation is less than 2.5% and vanishes at small and large values of  $q$ . The inset shows numerically determined  $S(z;q)$  for  $qR = 0.4$ . As  $z$  increases, this varies from the  $S_g(q)$  to the  $S_l(q)$  limits, showing a maximum near the origin (red circle).

hard spheres,  $\mu_h(\rho)$ , is considered an arbitrary function. To begin, we again consider systems with an Ising symmetry. In this case, the analysis of the square-gradient theory generalizes in a straightforward manner. Indeed, the central result (equation (4)) for the expansion of  $S(z;q)$  becomes

$$S(z;q) = S_b(q) \left( \gamma(z) + \lambda \sum_{n=1}^{\infty} \frac{\sigma}{\sigma_n} \mathcal{R}_n(z;q) \right) \quad (10)$$

which differs from equation (4) in only one regard: the first term on the right-hand side is modified to  $S_b(q)\gamma(z)$ , where  $\gamma(z) = \mu'_h(\rho_b)/\mu'_h(\rho(z))$  (see Supplementary Information).

The function  $\gamma(z)$  is larger than 1 for all finite  $z$ , but approaches 1 as  $T \rightarrow T_c$ , in which case, the results of the Sullivan model recover those of square-gradient theory. The effect of  $\gamma(z)$  is twofold. First, it leads to the enhancement of a bulk-like contribution, which is maximal at the origin. Second, it decays to 1 exponentially at large  $|z|$  and mixes with the explicit Goldstone mode term (controlled by  $\sigma_l$ ) to recover the asymptotic decay (equation (2)). With these provisos, the rest of the analysis is unchanged, including the classification of SRMs and fully integrable models, but now based on properties of the function  $\mu_h(\rho)$  rather than the potential  $\phi(\rho)$ . Most importantly, this allows us to understand the generalizations of the extremely accurate approximations, equations (7), (8) and (9) (which, we stress, also remain exact for some model functions  $\mu_h(\rho)$ ). These are now modified to

$$\frac{S(0;q)}{S_b(q)} \approx \gamma(0) + \frac{\Delta\rho\rho'(0)}{\sigma q^2 S_b(0)} \quad (11)$$

$$\frac{S_{\text{total}}(q)}{S_b(q)} \approx \int dz \gamma(z) + \frac{(\Delta\rho)^2}{\sigma q^2 S_b(0)} \quad (12)$$

and

$$\frac{G(0,0;q)}{G_b(0;q)} \approx \gamma(0)^2 + \frac{\rho'(0)^2}{\sigma q^2 G_b(0;0)} \quad (13)$$

The presence of the corrections introduced by the function  $\gamma(z)$  serves to underline again why there is no simple additive separation into bulk and excess quantities in the correlation function structure. Indeed, the enhancement effect means that neither  $S(0;q)$  nor  $G(0,0;q)$  approach their bulk values as  $q$  increases, not even when the Goldstone mode contribution is irrelevant.

Finally, we turn to the inclusion of liquid–gas asymmetry, which is now a relatively minor amendment. For example, the local structure factor at the origin (defined again as the location of the maximum of the density profile derivative) generalizes to

$$S(0;q) \approx f(q)\gamma_g S_g(q) + (1-f(q))\gamma_l S_l(q) + \frac{\Delta\rho\rho'(0)}{\sigma q^2} \left( f(q) \frac{S_g(q)}{S_g(0)} + (1-f(q)) \frac{S_l(q)}{S_l(0)} \right) \quad (14)$$

where  $\gamma_b = \mu'_h(\rho_b)/\mu'_h(\rho(0))$  and  $f(q) = \Delta\kappa_g(q)/(\Delta\kappa_g(q) + \Delta\kappa_l(q))$ ,  $\Delta\kappa_b(q) = \sqrt{\kappa_b^2 + q^2} - \kappa_b$  and  $\kappa_b$  is the inverse of the true correlation length in the bulk liquid ( $b=l$ ) and ( $b=g$ ) phases. This result encapsulates an accurate approximation for the weighting of different bulk-like and Goldstone mode contributions where there is an arbitrary liquid–gas asymmetry. In Fig. 4, we illustrate how well this expression works using the accurate Carnahan–Starling equation of state for  $\mu_h(\rho)$ . We stress that this approximation contains no free parameters.

### Summary

In this paper, we have shown that, by recognizing the presence of resonances, a very rich perspective emerges regarding correlation function structure for interfaces in systems with short-range forces.

Indeed, this allows us to essentially solve analytically for the correlation function in generalized van der Waals DFTs and eliminates the need for the introduction of a rigidity, highlighting properties that cannot be explained using such a simple mesoscopic concept. Our predictions for the local structure factor and correlation function can certainly be tested in Ising model simulation studies, similar to those described in ref.<sup>30</sup>, which have better statistics compared with molecular simulations. Our analysis of the resonances generalizes in a straightforward manner to more sophisticated non-local DFT treatments<sup>31</sup>. However, when the bulk correlation length is large, the predictions of the square-gradient theory will be accurate. It may also be possible to incorporate long-range forces, but similarly, they become irrelevant in the critical region<sup>32</sup>, and we expect that the local structure factor displays universal features that are correctly captured by models with short-range forces discussed here. Resonances will also occur for interfaces in binary liquid mixtures, and more generally still, will occur at other types of interface, such as the solid–liquid, even when a Goldstone mode is absent.

### Online content

Any methods, additional references, Nature Research reporting summaries, source data, statements of data availability and associated accession codes are available at <https://doi.org/10.1038/s41567-018-0361-z>.

Received: 23 August 2018; Accepted: 26 October 2018;

Published online: 10 December 2018

### References

- Zittartz, J. Microscopic approach to interfacial structure in Ising-like ferromagnets. *Phys. Rev.* **154**, 529–534 (1967).
- Wertheim, M. S. Correlations in the liquid–vapor interface. *J. Chem. Phys.* **65**, 2377–2381 (1976).
- Weeks, J. D. Structure and thermodynamics of the liquid–vapor interface. *J. Chem. Phys.* **67**, 3106–3121 (1977).
- Buff, F. P., Lovett, R. A. & Stillinger, F. H. Interfacial density profile for fluids in the critical region. *Phys. Rev. Lett.* **15**, 621–623 (1965).
- Aarts, D. G. A. L., Schmidt, M. & Lekkerkerker, H. N. W. Direct visual observation of thermal capillary waves. *Science* **304**, 847–850 (2004).
- Romero-Rochín, V., Varea, C. & Robledo, A. Microscopic expressions for interfacial bending constants and spontaneous curvature. *Phys. Rev. A* **44**, 8417–8420 (1991).
- Napiórkowski, M. & Dietrich, S. Structure of the effective Hamiltonian for liquid–vapor interfaces. *Phys. Rev. E* **47**, 1836–1849 (1993).
- Parry, A. O. & Boulter, C. J. Fluctuation theory for the wavevector expansion of the excess grand potential of a liquid–vapor interface and the theory of interfacial fluctuations. *J. Phys. Condens. Matter* **6**, 7199–7206 (1994).
- Robledo, A. & Varea, C. Interfacial width and shape fluctuations and extensions of the Gaussian model of capillary waves. *J. Stat. Phys.* **89**, 273–282 (1997).
- Mecke, K. R. & Dietrich, S. Effective Hamiltonian for liquid–vapor interfaces. *Phys. Rev. E* **59**, 6766–6784 (1999).
- Fradin, C. et al. Reduction in the surface energy of liquid interfaces at short length scales. *Nature* **403**, 871–874 (2000).
- Blokhuys, E. M., Kuipers, J. & Vink, R. L. C. Description of the fluctuating colloid–polymer interface. *Phys. Rev. Lett.* **101**, 086101 (2008).
- Blokhuys, E. M. On the spectrum of fluctuations of a liquid surface: from the molecular scale to the macroscopic scale. *J. Chem. Phys.* **130**, 014706 (2009).
- Parry, A. O., Rascón, C., Willis, G. & Evans, R. Pair correlation functions and the wavevector-dependent surface tension in a simple density functional treatment of the liquid–vapour interface. *J. Phys. Condens. Matter* **26**, 355008 (2014).
- Höfling, F. & Dietrich, S. Enhanced wavelength-dependent surface tension of liquid–vapor interfaces. *Europhys. Lett.* **109**, 46002 (2015).
- Chacón, E. & Tarazona, P. Capillary wave Hamiltonian for the Landau–Ginzburg–Wilson density functional. *J. Phys. Condens. Matter* **28**, 244014 (2016).
- Hernández-Muñoz, J., Chacón, E. & Tarazona, P. Capillary waves and the decay of density correlations at liquid surfaces. *Phys. Rev. E* **94**, 062802 (2016).
- Parry, A. O., Rascón, C. & Evans, R. The local structure factor near an interface; beyond extended capillary-wave models. *J. Phys. Condens. Matter* **28**, 244013 (2016).
- Macdowell, L. G. Capillary wave theory of adsorbed liquid films and the structure of the liquid–vapor interface. *Phys. Rev. E* **96**, 022801 (2017).
- Hernández-Muñoz, J., Chacón, E. & Tarazona, P. Capillary waves as eigenmodes of the density correlation at liquid surfaces. *J. Chem. Phys.* **148**, 084702 (2018).
- Helfrich, W. Elastic properties of lipid bilayers: theory and possible experiments. *Z. Naturforsch. C* **28**, 693–703 (1973).
- Evans, R., Henderson, J. R., Hoyle, D. C., Parry, A. O. & Sabeur, Z. A. Asymptotic decay of liquid structure: oscillatory liquid–vapour density profiles and the Fisher–Widom line. *Mol. Phys.* **80**, 755–775 (1993).
- Evans, R. The nature of the liquid–vapour interface and other topics in the statistical mechanics of non-uniform, classical fluids. *Adv. Phys.* **28**, 143–200 (1979).
- Rowlinson, J. S. & Widom, B. *Molecular Theory of Capillarity* (Clarendon, Oxford, 1982).
- Fernández, E. M., Chacón, E., Tarazona, P., Parry, A. O. & Rascón, C. Intrinsic fluid interfaces and nonlocality. *Phys. Rev. Lett.* **111**, 096104 (2013).
- Van Campen, N. G. Condensation of a classical gas with long-range attraction. *Phys. Rev.* **135**, 362–369 (1964).
- Percus, J. K. Current problems in statistical mechanics. *Trans. NY Acad. Sci.* **26**, 1062–1071 (1964).
- Sullivan, D. E. Van der Waals model of adsorption. *Phys. Rev. B* **20**, 3991–4000 (1979).
- Sullivan, D. E. Surface tension and contact angle of a liquid–solid interface. *J. Chem. Phys.* **74**, 2604–2615 (1981).
- Pang, L. J., Landau, D. P. & Binder, K. Simulation evidence for nonlocal interface models: two correlation lengths describe complete wetting. *Phys. Rev. Lett.* **106**, 236102 (2011).
- Rosenfeld, Y. Free-energy model for the inhomogeneous hard-sphere fluid mixture and density-functional theory of freezing. *Phys. Rev. Lett.* **63**, 980–983 (1989).
- Evans, R. & Henderson, J. R. Pair correlation function decay in models of simple fluids that contain dispersion interactions. *J. Phys. Condens. Matter* **21**, 474220 (2009).

### Acknowledgements

We are grateful to F. Höfling for providing his simulation results and for discussions. A.O.P. acknowledges the EPSRC, UK, for grant EP/L020564/1 (Multiscale Analysis of Complex Interfacial Phenomena). C.R. acknowledges the support of grant FIS2015-66523-P (MINECO/FEDER, UE).

### Author contributions

A.O.P. conceived the problem and subsequent joint theoretical development. C.R. performed joint theoretical development and numerical computations.

### Competing interests

The authors declare no competing interests.

### Additional information

Supplementary information is available for this paper at <https://doi.org/10.1038/s41567-018-0361-z>.

Reprints and permissions information is available at [www.nature.com/reprints](http://www.nature.com/reprints).

Correspondence and requests for materials should be addressed to C.R.

**Publisher's note:** Springer Nature remains neutral with regard to jurisdictional claims in published maps and institutional affiliations.

© The Author(s), under exclusive licence to Springer Nature Limited 2018

**Methods**

Methods, including the derivation of the relationship between  $S(z;q)$  and  $G(0,z;q)$ , the classification of SRMs and the explicit solution for  $G(z,z';q)$  in a model with an infinite hierarchy of resonances, can be found in the Supplementary Information.

**Data availability**

The data that support the plots within this paper and other findings of this study are available from the corresponding author upon reasonable request.